Editors' Suggestion

Magnetic property changes of NdGa upon hydrogen absorption

Johan Cedervall,[1,*] Vitalii Shtender,[1] Pascal Manuel,[2] Vladimir Pomjakushin,[3] Roland Mathieu,[4] Ulrich Häussermann,[5] and Mikael S. Andersson[1,†]

[1]*Department of Chemistry - Ångström Laboratory, Uppsala University, Box 538, SE-751 21 Uppsala, Sweden*
[2]*ISIS Pulsed Neutron & Muon Facility, Rutherford Appleton Laboratory, Harwell Campus, OX11 0QX, United Kingdom*
[3]*Laboratory for Neutron Scattering and Imaging, Paul Scherrer Institut, 5232 Villigen, Switzerland*
[4]*Department of Materials Science and Engineering, Uppsala University, Box 35, 751 03 Uppsala, Sweden*
[5]*Department of Materials and Environmental Chemistry, Stockholm University, 106 91 Stockholm, Sweden*

(Received 16 February 2024; revised 4 April 2024; accepted 5 April 2024; published 23 April 2024)

Rare earth monogallide (REGa) Zintl phases are attractive for their properties in hydrogen storage and magnetic cooling. However, the magnetic effects upon hydrogen additions in REGa are not well understood. This study aims to explore the magnetic effects in $REGaH_x$ using SQUID magnetometry and neutron powder diffraction. To avoid challenges due to absorption and high incoherent scattering in the neutron diffraction experiments, the compound $NdGaD_x$ ($x = 0$, 0.9, or 1.6) was chosen for examination. It was found that NdGa exhibits two ferromagnetic structures below the Curie temperature of 42 K. Just below 42 K the magnetic moments are oriented along the crystallographic c axis, and at 20 K a spin reorientation occurs where the moments turn $\sim 30^\circ$ toward the a axis. Upon partial deuteration ($x = 0.9$), the magnetization decreases and two magnetic phases are observed, one intermediate incommensurate phase, and one canted ferromagnetic phase with the net magnetization aligning along the b axis. For the full deuteride ($x = 1.6$) only one incommensurate magnetic phase is observed at low temperatures. Magnetometry also reveals that there are no isotope effects when absorbing H or D. The absorption of H or D changes the Nd-Nd distances as well as the electronic structure, which results in a drastic change in the magnetic properties as compared to NdGa.

DOI: 10.1103/PhysRevB.109.134434

I. INTRODUCTION

Zintl phases of the rare earth (RE) monogallides (REGa) have recently attracted attention due to their potential use as magnetocaloric materials [1–3]. They are in general ferromagnetic and, going through the lanthanide series from PrGa to GdGa, the Curie temperature (T_C) increases from about 30 K to a maximum of 190 K [4–6]. From GdGa to TmGa, (T_C) decreases from about 190 K down to about 14 K [4–6]. By forming hydrides ($REGaH_x$) the magnetic properties of several of these compounds have been shown to change drastically, e.g., as in NdGa and GdGa where the dominating type of interaction goes from ferromagnetic to antiferromagnetic upon hydrogenation [7,8]. These intriguing changes in the magnetic order have to date primarily been studied by magnetometry, as well as for fully hydrogenated hydrides ($REGaH_{1.67}$, highest hydrogen content stable at ambient pressures). To better understand the impact that hydrogen incorporation has on the magnetism of these compounds, detailed magnetic structure characterizations are required and one of the best tools for determining the magnetic structure is neutron diffraction. However, due to the large neutron absorption cross section for Gd, neutron scattering experiments on Gd containing samples are challenging and $NdGaH_x$ thus lends itself as a better candidate for such a study.

NdGa crystallizes in the CrB structure type and has discrete Nd and Ga layers that are fully occupied as shown in Fig. 1(a) [9]. The unit cell parameters are 4.4329(12) Å, 11.246(3) Å, and 4.1735(11) Å for a, b, and c, respectively [10]. It has been shown that NdGa absorbs hydrogen on two different positions in the structure, and the absorption occurs in two discrete steps [10]. In the first step, a monohydride is formed, Fig. 1(b), where H has a tetrahedral coordination to Nd. The added H results in a slight increase of the unit cell volume, mostly because of an expansion of the b axis, the unit cell parameters for the hydrides (deuterides) can be found in Ref. [10]. Upon full hydrogenation, a superstructure is formed which has a tripled a axis compared to the structure of NdGa. The superstructure splits all atomic sites from NdGaH, and the extra H forms covalent bonds with Ga [10]. The H-Ga bonds form a chain in the center of the unit cell and Ga-H-Ga trimers close to the (010) plane, Fig. 1(c). Given the high incoherent neutron scattering cross section of H, D is used instead in the study to simplify the neutron diffraction experiments.

In this article, a detailed study of the magnetism of $NdGaD_x$ ($x = 0$, 0.9 or 1.6) using SQUID magnetometry and neutron powder diffraction (NPD) is presented. Given the high incoherent neutron scattering cross section of H, D

*johan.cedervall@kemi.uu.se
†mikael.andersson@kemi.uu.se

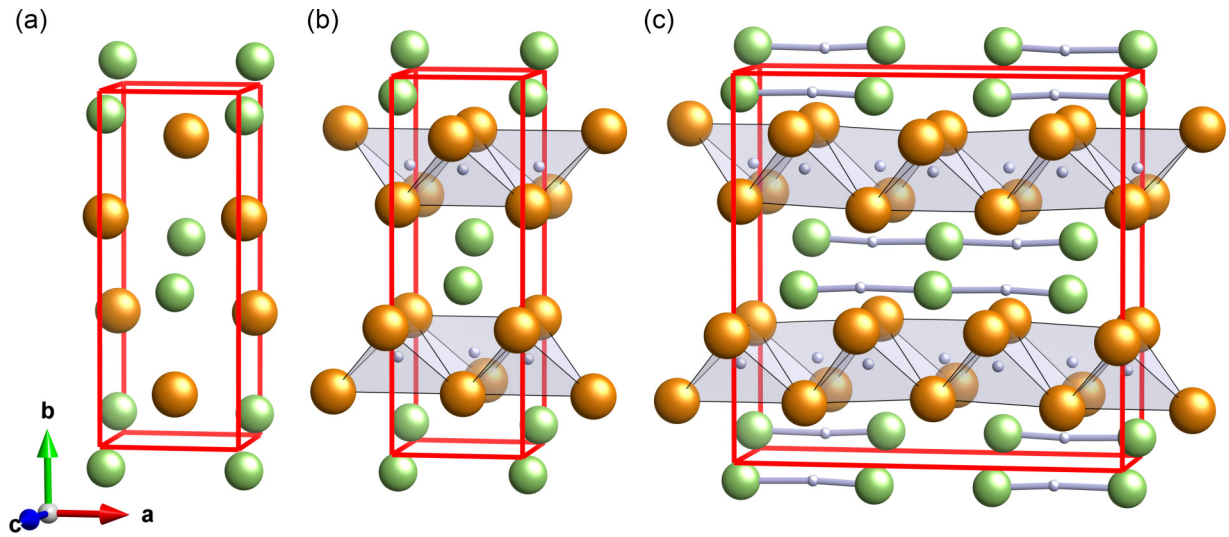

FIG. 1. Nuclear structure models for (a) NdGa, (b) NdGaH, and (c) $NdGaH_{1.67}$. Nd, Ga, and H are represented with orange, green, and gray spheres, respectively. The figure is based on data reported in Ref. [10].

is used instead in the study to simplify the neutron diffraction experiments. The results show that NdGa exhibits two ferromagnetic phases, one between 42 K and 20 K, as well as one below 20 K. At 42 K the magnetic moment of Nd orders ferromagnetically along the crystallographic c axis, while at around 20 K a $\sim 30^{\circ}$ rotation of the magnetic moment of Nd toward the a axis occurs. The results also show that $NdGaD_{0.9}$ exhibits two magnetic phases, one incommensurate phase (5–14 K) and a canted ferromagnetic phase below 5 K, while $NdGaD_{1.6}$ exhibits an incommensurate magnetic phase below 4 K.

II. METHODS

A. Synthesis

The NdGa alloy was synthesized by arc melting stoichiometric amounts of Nd (Smart-elements, purity 99.9%) and Ga (99.999%) under argon atmosphere, however, to avoid $NdGa_2$-impurities 1% excess of Nd was used. The sample was wrapped in Ta foil and placed in a stainless-steel tube and annealed in a muffle furnace at 1170 K for five days. After the annealing the sample was quenched in cold water. Full deuterides were produced in a stainless-steel autoclave at 570 K using deuterium pressures of 25 bar. The partial deuteride was made by partially desorbing the full deuteride. Slight vacancies on D gives a total chemical formula of $NdGaD_{0.91(1)}$ and $NdGaD_{1.59(1)}$, which for simplicity will be shortened to $NdGaD_{0.9}$ and $NdGaD_{1.6}$, respectively. Corresponding hydrides (NdGaH and $NdGaH_{1.6}$) were also synthesized to allow verification that deuterides have the same magnetic properties as the hydrides. A full description of the synthesis procedure can be found in Ref. [10] for both the deuterides as well as corresponding hydrides. The samples used here are the same as in Ref. [10].

B. Magnetometry

Magnetization (M) measurements were performed as a function of temperature (T) or applied magnetic field (H) using a Quantum Design MPMS SQUID Magnetometer. M vs T measurements were performed using both a small applied magnetic field (4 kA/m) to accurately determine the magnetic phase transitions, and using a large applied magnetic field (80 kA/m for NdGa and 800 kA/m for $NdGaD_{0.9}$ and $NdGaD_{1.6}$) in order to estimate the effective magnetic moment (μ_{eff}) and the Curie-Weiss temperature (θ_{CW}) from Curie-Weiss (CW) fits of the data. M vs H measurements were performed at a few select temperatures using an applied magnetic field of ± 4000 kA/m to study the field dependence.

C. Neutron powder diffraction

To elucidate the magnetic structures, neutron powder diffraction (NPD) was employed using the instruments HRPT [11] and WISH [12,13] at SINQ (PSI, Villigen Switzerland) and ISIS Neutron and Muon Source (Didcot, UK), respectively. The experiments at HRPT used a Ge monochromator (reflection 511), giving a wavelength of 1.886 Å. NdGa was measured at 1.5, 30, 55, and 100 K using HRPT, while $NdGaD_{0.9}$ and $NdGaD_{1.6}$ were measured using WISH at 1.5 and 20 K, as well as at 1.5, 7, and 20 K, respectively.

The obtained diffraction data were analyzed using the Rietveld method [14] implemented in the software FullProf [15]. In the refinements, several structure parameters, including the atomic positions, atomic displacement, and D occupancies, were allowed to vary. For the commensurate magnetic structures all possible magnetic space groups (MSGs) were evaluated with k-SUBGROUPSMAG [16] and tested against the diffraction data below (T_C). All structure figures were made using the software VESTA [17].

III. RESULTS

A. Magnetometry

Low-field zero-field-cooled (ZFC) magnetization as a function of temperature measurement for NdGa, $NdGaD_{0.9}$, and $NdGaD_{1.6}$ are presented in Fig. 2. In the figure it can be

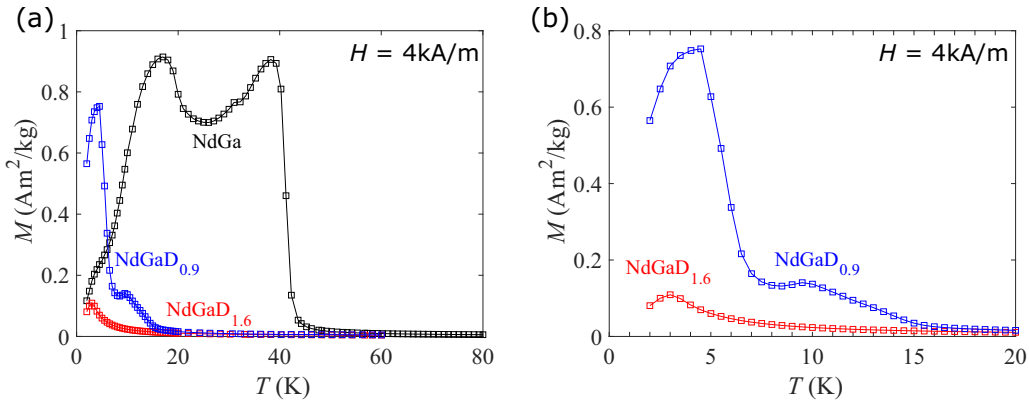

FIG. 2. ZFC magnetization as a function of temperature using a field of H = 4kA/m for (a) NdGa, $NdGaD_{0.9}$, and $NdGaD_{1.6}$ in the temperature range of 2–80 K and (b) in the range 2–20 K.

seen that NdGa exhibits two clear magnetic features, one at ∼42 K and a second at approximately 20 K. The feature at about 42 K is identified as the ferromagnetic transition temperature for NdGa [5–7,18]. The feature at ∼20 K has been discussed in a previous Mössbauer study, which suggests that the feature corresponds to a spin reorientation in the *ac* plane [18]. Comparing NdGa to $NdGaD_x$ ($x = 0.9$ or 1.6) it can be noted that the transition temperatures decrease significantly with increasing amounts of deuterium. For $NdGaD_{0.9}$ two features can be observed, one below 14 K and one below 5 K, while for $NdGaD_{1.6}$ only one feature below 4 K can be seen. A comparison between the low-field ZFC(T) measurements of $NdGaH_x$ and $NdGaD_x$ is shown in Fig. S1 in the Supplemental Material (SM) [19]. The ZFC(T) data suggests that the magnetic properties are isotope independent with regards to H and D. However, a small shift in the transition temperature is seen for NdGaH as compared to $NdGaD_{0.9}$. This is attributed to a possible slight difference in the amount of absorbed H/D between the two samples.

To investigate the magnetic interactions in NdGa, $NdGaD_{0.9}$, and $NdGaD_{1.6}$ high-field magnetization as a function of temperature measurements were made. The data corresponding to the paramagnetic regime was fitted to the Curie-Weiss law [$M/H = C/(T - \theta_{CW})$] and the results are presented in Table I, as well as in Fig. S2 in the SM. For NdGa, $\theta_{CW} \sim 38.9$ K indicates ferromagnetic interactions, while for $NdGaD_{0.9}$ and $NdGaD_{1.6}$, $\theta_{CW} \sim -11.8$ K and $\theta_{CW} \sim -14.9$ K, respectively, thus indicate antiferromagnetic interactions. The theoretical value for the effective magnetic moment of Nd^{3+} is 3.62 μ_B [20], which is close to the experimental values determined here for NdGa (3.3 μ_B), $NdGaD_{0.9}$ (3.5 μ_B), and $NdGaD_{1.6}$ (3.2 μ_B), suggesting a Nd^{3+} oxidation state. The μ_{eff} values for NdGa and $NdGaD_{1.6}$ agree fairly well with previous studies [7,21], while no other magnetic studies have been conducted for $NdGaD_{0.9}$. For NdGa the θ_{CW} value is in good agreement with the literature [7,21], while for $NdGaD_{1.6}$ the $\theta_{CW} = -14.9$ K found here deviates slightly from the value of −22.4K in Ref. [7].

TABLE I. Transition temperatures T_1 and T_2, effective magnetic moment (μ_{eff}), and the Curie-Weiss temperature (θ_{CW}) for NdGa, $NdGaD_{0.9}$, and $NdGaD_{1.6}$. For NdGa, T_1 corresponds to the Curie temperature (T_C), while T_2 corresponds to the spin-reorientation temperature.

Sample	T_1 (K)	T_2 (K)	μ_{eff} (μ_B)	θ_{CW} (K)
NdGa	42	20	3.3	38.9
$NdGaD_{0.9}$	14	5	3.5	−11.8
$NdGaD_{1.6}$	4		3.2	−14.9

The magnetization as a function of applied magnetic field measurements are presented in Fig. 3. For NdGa it can be noted that magnetization increases rapidly with an applied magnetic field for both measurements made at 2 K and at 30 K (see the inset of Fig. 3). However, the approach to saturation is different between the two temperatures. At 2 K, NdGa reaches a plateau value with only a slight increase in the magnetization upon application of a larger magnetic field, while at 30 K the approach to saturation exhibits a much more sloped shape and does not reach a plateau value even at applied magnetic fields of 4000 kA/m. Comparing the magnetization at 4000 kA/m for the measurements performed at 2 K and 30 K for NdGa it

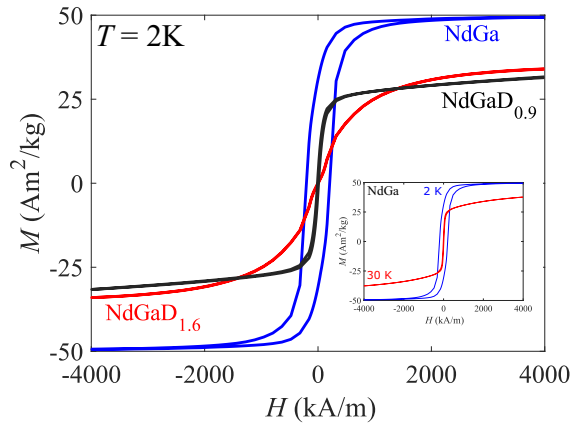

FIG. 3. Magnetization as a function of applied magnetic field for NdGa, $NdGaD_{0.9}$, and $NdGaD_{1.6}$ at 2 K. The inset shows the magnetization as a function of applied magnetic field for NdGa at 2 and 30 K.

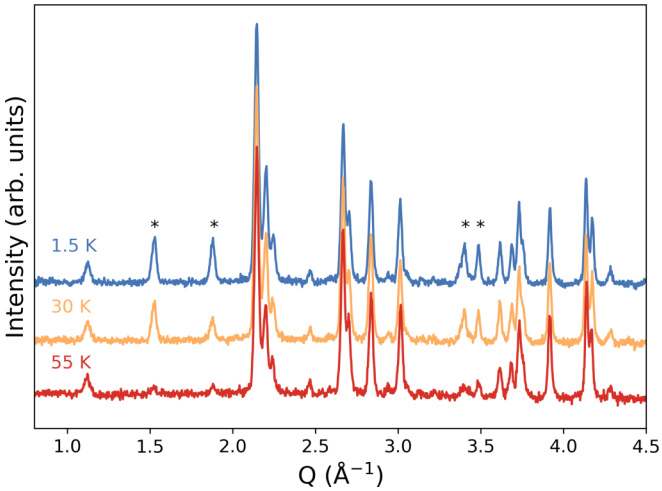

FIG. 4. Neutron powder diffraction patterns for NdGa below 4.5 Å^{-1} showing the additional magnetic intensities which appear when cooling below T_C. The peaks with the strongest magnetic contributions are marked with *. $\lambda = 1.886$ Å.

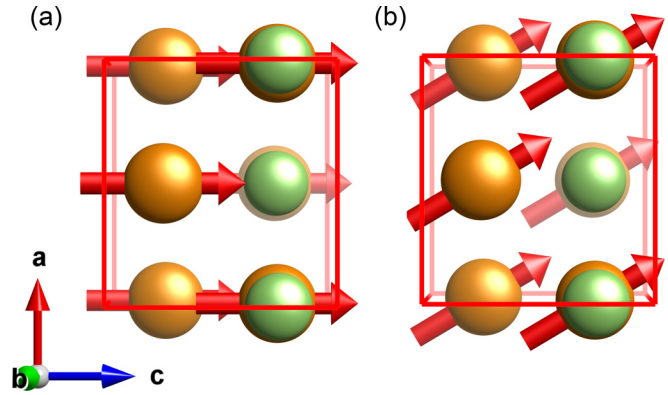

FIG. 5. Refined magnetic structure models for NdGa at (a) 30 K in the MSG $Cm'c'm$ and (b) 1.5 K in the MSG $C2'/c'$.

can be seen that the magnetization at 30 K decreases to about 75% of the magnetization at 2 K. It can also be noted that the magnetization of ∼50 Am^2/kg at 2 K and 4000 kA/m is slightly smaller than the ∼55 Am^2/kg at 6 K and 4000 kA/m in Ref. [7] and smaller than the ∼60 Am^2/kg at 5 K and 4000 kA/m in Ref. [3]. The differences in magnetization is attributed to the relatively large uncertainty in weight of the sample due to the small sample weight (∼1 mg). Similar to NdGa, the magnetization for $NdGaD_{0.9}$ at 2 K increases rapidly upon the application of an applied magnetic field. However, the magnetization for $NdGaD_{0.9}$ does not reach a plateau at higher fields and has a much more pronounced slope than NdGa. For $NdGaD_{1.6}$ the magnetization increases much more gradually upon application of an applied magnetic field as compared to NdGa and $NdGaD_{0.9}$, i.e., the M vs H curve has a much more rounded shaped. Similar to $NdGaD_{0.9}$ no plateau value is reached at higher fields for $NdGaD_{1.6}$.

B. Magnetic structures

1. NdGa

The two magnetic transitions observed for NdGa with low field magnetization measurements were examined with NPD at 1.5 and 30 K using the instrument HRPT. The diffraction patterns below (T_C) reveal peaks with increased intensities, especially below ∼3.5 Å^{-1}, as shown in Fig. 4. The positions of the magnetic intensities are on existing nuclear diffraction positions showing that the propagation vector $\mathbf{k} = (0\ 0\ 0)$. This $\mathbf{k}$ vector is not surprising given that the Curie-Weiss fit indicated FM interactions. Upon evaluation of the possible magnetic space groups, matching intensities were found at 30 K for the MSG $Cm'c'm$. All magnetic moments are aligned along the c direction and have a refined magnetic moment of 2.5(1) μ_B/Nd atom, visualized in Fig. 5(a). This is in good agreement with the single crystal magnetometry study of Ref. [21], which shows a high magnetization along the crystallographic c direction at 40 K. The unit cell parameters when cooling through (T_C), are affected by the magnetization of the compound, where an increase is seen in the ab plane and a slight decrease of the b axis. The change in unit cell parameters strongly correlates with the magnetic spin directions of Nd. The refinements used to determine the magnetic structures are shown in Fig. S5 in the SM [19].

At 1.5 K, below the spin reorientation temperature of 20 K, NPD reveals a canting of the magnetic moments toward the a axis. The magnetic space group changes upon cooling to $C2'/c'$ and the value of the magnetic moment were refined to 3.2(1) μ_B/Nd atom with a tilting angle of 30.5(2)° away from the c axis, Fig. 5(b). The tilt is clearly visible from the extra intensity on the reflection 021 (Q = 1.88 Å^{-1}), which have a strong contribution to the a direction of the magnetic moment. The refined model is in good agreement with the single crystal magnetometry study of Ref. [21], which shows high magnetization along two crystallographic directions (a and c) at 2 K. The magnetic spin reorientation presented here are in agreement with the previous Mössbauer study [18]. The MSG $C2'/c'$ is a subgroup to $Cm'c'm$ which means that the spin reorientation is of second order, according to Landau theory [22].

2. $NdGaD_{0.9}$

The deuterated samples were studied with NPD using the instrument WISH to evaluate the magnetic behavior. For $NdGaD_{0.9}$, there are two magnetic arrangements, one at low temperatures (<5 K), and one at intermediate temperatures (5–14 K). The low temperature phase was examined at 1.5 K and was found to be commensurate, with $\mathbf{k} = (0\ 0\ 0)$. The MSG that gives the best agreement with the experimental diffraction patterns in the refinements is $Cm'c2_1'$, which gives a model with the magnetic moments oriented ferromagnetically along the b axis, but with a slight antiferromagnetic canting in the c direction. The antiferromagnetic canting is in good agreement with the antiferromagnetic interactions suggested from the CW fit as well as the reduction in magnetization at 4000 kA/m and the increased slope above 1000 kA/m as compared to NdGa. However, the refinement is only improved slightly by including the canting which suggests that it might not be needed in the magnetic structure model. A model without canting is shown in Fig. S4 (SM) [19]. The total amplitude of the magnetic moments were refined to

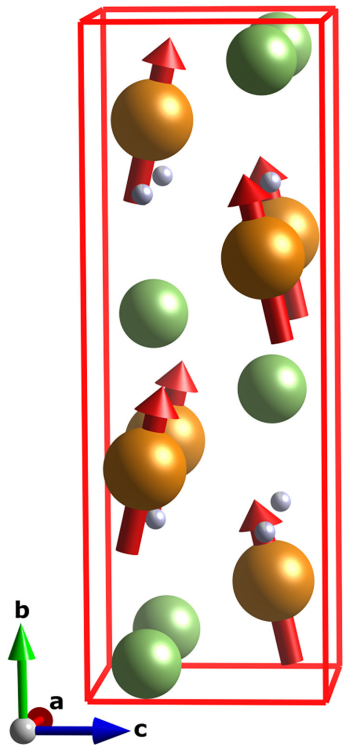

FIG. 6. Refined magnetic structure model for $NdGaD_{0.9}$ at 1.5 K in the MSG $Cm'c2'_1$.

1.7(1) μ_B, with an antiferromagnetic canting toward the c direction of 13(3)°. The magnetic structure is visualized in Fig. 6, and the refinements can be found in the SM (Fig. S6). There is no group-subgroup relation between $Cm'c2'_1$ and the MSGs describing the structures found for NdGa; consequently, the addition of D alters the Nd-Nd interactions and changes the magnetic symmetries in the structure. The difference between all commensurate magnetic structures are shown in the SM (Fig. S3).

The magnetic behavior at intermediate temperatures (examined at 7 K) are found to originate from an incommensurate magnetic structure. This is clearly shown from new peaks at 0.27 $Å^{-1}$ and satellites around the nuclear peaks, Fig. S7 in the SM. The magnetic peaks were used to investigate the magnetic propagation vector, **k**, using the software **k** search in the FullProf Suite [15]. At first, all special propagation vectors were tested, however, they were unable to describe the peak positions of the magnetic reflections. The **k** vectors that had the best fit were **k** = (0.15(3) 0.25(1) 0.06(4)), but all the tested models fails to properly describe the magnetic reflections in the experimental powder patterns. In the model that best describes the data, the magnetic moments are oriented along the crystallographic b axis, with a sinusoidal propagation of the magnitudes of the magnetic spins. The attempted magnetic structure refinement can be found in Fig. S8 in the SM [19].

3. $NdGaD_{1.6}$

Below the magnetic transition temperature for $NdGaD_{1.6}$, several new peaks appear in the powder diffraction pattern, Fig. S7 in the SM [19]. It is clearly an incommensurate structure, and by using a propagation vector of **k** = (0.48(4) 0.27(2) 0.27(2)) most of the new peaks can be described. The behavior from $NdGaD_{0.9}$ suggests that this incommensurate structure is an intermediate phase during the ordering process of $NdGaD_{1.6}$ and by further cooling, a commensurate magnetic structure may appear. However, to fully explore this, experiments below 1.5 K and possibly in the milikelvin regime are required.

IV. DISCUSSION

A. Magnetic property changes

The magnetometry and the NPD experiments show that NdGa exhibits two ferromagnetic phases, one between 42 K and 20 K as well as one below 20 K. The two phases have different directions of the magnetic spins, but the magnetic symmetries are related, giving a clear second order spin reorientation. The effective magnetic moment extracted from Curie-Weiss analysis suggest that Nd has a Nd^{3+} oxidation state. For a Nd^{3+} oxidation state, the theoretical Nd magnetic moment is ∼3.3 μ_B/Nd atom [20], in good agreement with the 3.2(1) μ_B/Nd atom found from NPD at 1.5 K. For $NdGaD_{0.9}$, the magnetic interactions are of an antiferromagnetic type according to the CW fits, and two magnetic transitions can be seen in the temperature dependent magnetization measurements. The two transitions can also be observed with NPD, and in the temperature range 5–14 K the spin interactions are of a complex ordering, with an antiferromagnetic incommensurate structure. However, at low temperatures (<5 K), the magnetic structure can be described as a canted ferromagnet, with a net magnetic moment of 1.7 μ_B/Nd atom. The ferromagnetic component of the spin correlates well with the field dependent magnetization behavior. Both magnetometry and NPD shows one magnetic transition in $NdGaD_{1.6}$, with nonferromagnetic interactions, in the measured temperature range. An incommensurate magnetic structure is suggested from NPD, which is in agreement with the magnetometry measurements.

B. Correlation with Nd-Nd distances

During deuteration (hydrogenation) of $NdGaD_x$ ($0 < x < 1$), the deuterium is absorbed by NdGa into the tetrahedral site formed by four Nd atoms, while for $NdGaD_x$ ($1 < x < 1.6$) the additional deuterium is absorbed into the trigonal bipyramidal site formed by three Nd atoms and two Ga atoms; see Fig. 7. The nuclear structures for NdGa and its hydrides are very robust and only very small changes (<0.5%) of the unit cell parameters and atomic positions occur between the highest and lowest temperatures. For NdGa the Nd-Nd distance within the tetrahedron (d_1) is 3.895(1) Å, while the closes Nd-Nd distance between two tetrahedra (d_2) is 3.814(1) Å. For $NdGaD_{0.9}$, d_1 becomes significantly shorter [3.734(1) Å] while d_2 becomes significantly longer [4.238(2) Å]. A summary of all of the Nd-Nd distances is given in Table II. Comparing magnetic structures for NdGa and $NdGaD_{0.9}$ at 1.5 K, it can be seen that the magnetic moment of Nd goes from being aligned in the ac plane for NdGa, i.e., in the plane parallel to the layer

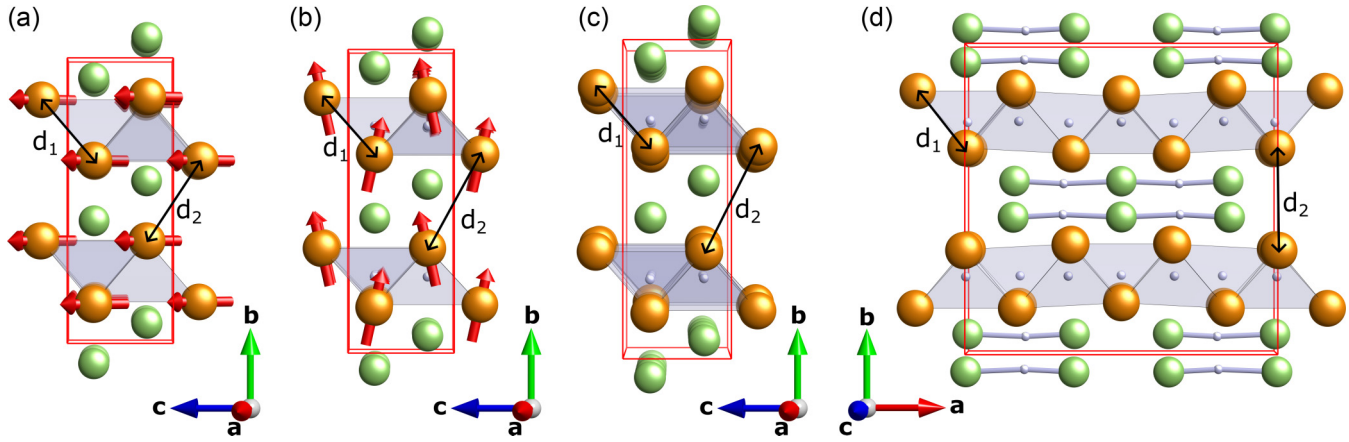

FIG. 7. Structures for $NdGaD_x$ at 1.5 K highlighting the Nd-Nd distances within the thetrahedron (d_1) and between different tetrahedra (d_2) for (a) NdGa, (b) $NdGaD_{0.9}$, (c) $NdGaD_{1.6}$ in the *bc* plane, and (d) $NdGaD_{1.6}$ in the *ba* plane.

formed by the Nd tetrahedra, to having its largest component aligned along the *b* direction, i.e., perpendicular to the layer formed by the Nd-tetrahedra; see Figs. 7(a) and 7(b). In addition to the changes of the magnetic structure, the transition temperature for $NdGaD_{0.9}$ is also significantly lowered. Assuming that the dominating interaction mechanism for NdGa is the Ruderman-Kittel-Kasuya-Yosida (RKKY) [23–25], as suggested for GdGa [26], and that RKKY remains the dominating interacting mechanism for $NdGaD_{0.9}$, the large changes of the Nd-Nd distances are likely to drastically alter the interaction strength and possibly introduce significant antiferromagnetic interactions. While this agrees well with the observed changes in the magnetic structure it is also possible that these changes stem from a change in the electronic structure upon absorption of H/D into the Nd-tetrahedra since, as shown in Ref. [7], H absorption is accompanied with a shift of the Fermi level toward a pseudogap in the density of states.

Upon further deuteration of $NdGaD_{0.9}$ to $NdGaD_{1.6}$, d_1 increases slightly to 3.748(1) Å, while d_2 continues to increase significantly to 4.564(2) Å. These changes in the Nd-Nd distances also coincide with a large change in the transition temperature and similar to $NdGaD_{0.9}$ the distance changes, assuming RKKY interactions, could account for the observed changes in the magnetic properties. However, as in the case of $NdGaD_{0.9}$, electronic structure changes from introduction of deuterium into the trigonal bipyramidal could also be the cause of the magnetic property changes.

TABLE II. Shortest Nd-Nd distances at RT within the tetrahedron (d_1) and between different tetrahedra (d_2). Errors are given within the parenthesis.

Sample	d_1 (Å)	d_2 (Å)
NdGa	3.895(1)	3.814(1)
$NdGaD_{0.9}$	3.734(1)	4.238(2)
$NdGaD_{1.6}$	3.748(1)	4.564(2)

V. CONCLUSIONS

In this study, magnetometry and neutron powder diffraction have been used to reveal the magnetic properties of NdGa and explore the effects on the magnetism by hydrogen insertion. The magnetic ordering for NdGa occurs at 42 K, where the magnetic moments align along the crystallographic *c* axis (MSG $Cm'c'm$), and undergoes a second order spin rotation at 20 K (MSG $C2'/c'$). The size of the magnetic moments extracted from neutron powder diffraction at 1.5 K are well in agreement with the theoretical value for Nd^{3+}. Upon insertion of deuterium, the magnetic transition temperature drops gradually with an increasing amount of D. For the partially deuterated sample ($NdGaD_{0.9}$), a canted ferromagnetic structure is observed at low temperatures (<5 K), while an intermediate incommensurate magnetic state is found between 5 K and 14 K. For $NdGaD_{1.6}$, only one magnetic state is found in the examined temperature range, which has an incommensurate magnetic structure below 4 K. The isotope effects with H/D absorption were also investigated, but no clear difference was found by using the heavier D instead of H.

In summary, the addition of H/D to NdGa alters the Nd-Nd interactions in a way that decreases the magnetic correlations, rotates the spins, and lowers the magnetization. The underlying reason is likely related to changes in the RKKY interactions between the magnetic Nd-atoms due to changes in the Nd-Nd distance and the electronic structure. To verify these findings, further studies using first-principles calculations are needed.

ACKNOWLEDGMENTS

Financial support from the Swedish Research Council (VR), Grants No. 2019-00645 and No. 2017-06345, and ÅForsk Foundation Grants No. 21-196, No. 21-453 and No. 22-378 are gratefully acknowledged. Experiments at the ISIS Neutron and Muon Source were supported by a beamtime allocation RB2220206 from the Science and Technology Facilities Council. This work is based on experiments performed at the Swiss spallation neutron source SINQ, Paul Scherrer Institute, Villigen, Switzerland. M.S.A. acknowledges support from the Göran Gustafsson Foundation.

[1] J. Zhang, J. Luo, J. Li, J. Liang, Y. Wang, L. Ji, Y. Liu, and G. Rao, Magnetic properties and magnetocaloric effect of GdGa compound, J. Alloys Compd. **469**, 15 (2009).

[2] J. Chen, B. Shen, Q. Dong, F. Hu, and J. Sun, Large reversible magnetocaloric effect caused by two successive magnetic transitions in ErGa compound, Appl. Phys. Lett. **95**, 132504 (2009).

[3] X. Zheng, J. Xu, S. Shao, H. Zhang, J. Zhang, S. Wang, Z. Xu, L. Wang, J. Chen, and B. Shen, Large magnetocaloric effect of NdGa compound due to successive magnetic transitions, AIP Adv. **8**, 056425 (2018).

[4] B. Barbara, V. N. Nguyen, and E. Siaud, Magnetic properties of equiatomic Ga-rare-earth metal compounds, Compt. Rend. **274**, 1053 (1972).

[5] H. Fujii, N. Shohata, T. Okamoto, and E. Tatsumoto, Magnetic properties of rare earth gallium compounds RGa, J. Phys. Soc. Jpn. **31**, 1592 (1971).

[6] N. Shohata, Magnetic properties of rare earth gallium intermetallic compounds, J. Phys. Soc. Jpn. **42**, 1873 (1977).

[7] J. Ångström, R. Johansson, T. Sarkar, M. H. Sørby, C. Zlotea, M. S. Andersson, P. Nordblad, R. H. Scheicher, U. Häussermann, and M. Sahlberg, Hydrogenation-induced structure and property changes in the rare-earth metal gallide NdGa: Evolution of a $[GaH]^{2-}$ polyanion containing Peierls-like Ga–H chains, Inorg. Chem. **55**, 345 (2016).

[8] R. Nedumkandathil, V. F. Kranak, R. Johansson, J. Ångström, O. Balmes, M. S. Andersson, P. Nordblad, R. H. Scheicher, M. Sahlberg, and U. Häussermann, Hydrogenation induced structure and property changes in GdGa, J. Solid State Chem. **239**, 184 (2016).

[9] A. E. Dwight, J. W. Downey, and R. A. Conner Jnr, Equiatomic compounds of Y and the lanthanide elements with Ga, Acta Crystallogr. **23**, 860 (1967).

[10] V. Shtender, J. Cedervall, G. Ek, C. Zlotea, M. S. Andersson, P. Manuel, M. Sahlberg, and U. Häussermann, Revisiting the hydrogenation behavior of NdGa and its hydride phases, J. Appl. Crystallogr. **57**, 248 (2024).

[11] P. Fischer, G. Frey, M. Koch, M. Könnecke, V. Pomjakushin, J. Schefer, R. Thut, N. Schlumpf, R. Bürge, U. Greuter, S. Bondt, and E. Berruyer, High-resolution powder diffractometer HRPT for thermal neutrons at SINQ, Phys. B: Condens. Matter **276-278**, 146 (2000).

[12] L. C. Chapon, P. Manuel, P. G. Radaelli, C. Benson, L. Perrott, S. Ansell, N. J. Rhodes, D. Raspino, D. Duxbury, E. Spill, and J. Norris, Wish: The new powder and single crystal magnetic diffractometer on the second target station, Neutron News **22**, 22 (2011).

[13] J. Cedervall, P. Manuel, M. Andersson, V. Shtender, and U. Haussermann, Hydrogen induced magnetic structure changes in $NdGaD_x$, STFC ISIS Neutron and Muon Source (2022), doi: 10.5286/ISIS.E.RB2220206.

[14] H. M. Rietveld, A profile refinement method for nuclear and magnetic structures, J. Appl. Crystallogr. **2**, 65 (1969).

[15] J. Rodríguez-Carvajal, Recent advances in magnetic structure determination by neutron powder diffraction, Phys. B: Condens. Matter **192**, 55 (1993).

[16] J. Perez-Mato, S. Gallego, E. Tasci, L. Elcoro, G. de la Flor, and M. Aroyo, Symmetry-based computational tools for magnetic crystallography, Annu. Rev. Mater. Res. **45**, 217 (2015).

[17] K. Momma and F. Izumi, *VESTA*: a three-dimensional visualization system for electronic and structural analysis, J. Appl. Crystallogr. **41**, 653 (2008).

[18] N. Delyagin, V. Krylov, and I. Rozantsev, The magnetic spin-reorientation transitions in the RGa (R=rare earth) intermetallic compounds studied by measurements of the hyperfine interactions of the ^{119}Sn probe atoms, J. Magn. Magn. Mater. **308**, 74 (2007).

[19] See Supplemental Material at http://link.aps.org/supplemental/10.1103/PhysRevB.109.134434 for additional magnetometry and neutron diffraction data.

[20] N. W. Ashcroft and N. D. Mermin, *Solid State Physics* (Cengage Learning, 1976).

[21] Y. Jia, T. Namiki, S. Kasai, L. Li, and K. Nishimura, Magnetic anisotropy and large low field rotating magnetocaloric effect in NdGa single crystal, J. Alloys Compd. **757**, 44 (2018).

[22] D. P. Landau, Theory of magnetic phase transitions, *Handbook of Magnetism and Advanced Magnetic Materials* (Wiley, 2007).

[23] M. A. Ruderman and C. Kittel, Indirect exchange coupling of nuclear magnetic moments by conduction electrons, Phys. Rev. **96**, 99 (1954).

[24] T. Kasuya, A theory of metallic ferro- and antiferromagnetism on Zener's model, Prog. Theor. Phys. **16**, 45 (1956).

[25] K. Yosida, Magnetic properties of Cu-Mn alloys, Phys. Rev. **106**, 893 (1957).

[26] X. Liu and Z. Altounian, Exchange interaction in GdGa from first-principles, Phys. B: Condens. Matter **406**, 710 (2011).